

# CW ENERGY RECOVERY OPERATION OF AN XFEL \*

J. Sekutowicz<sup>1,4</sup>, S. A. Bogacz<sup>1</sup>, M. Ferrario<sup>2</sup>, I. Ben-Zvi<sup>3</sup>, J. Rose<sup>3</sup>,  
P. Colestock<sup>5</sup>, D. Douglas<sup>1</sup>, P. Kneisel<sup>1</sup>, W.-D. Möller<sup>4</sup>, B. Petersen<sup>4</sup>, D. Proch<sup>4</sup>,  
J. B. Rosenzweig<sup>6</sup>, L. Serafini<sup>2</sup>, S. Simrock<sup>4</sup>, T. Srinivasan-Rao<sup>3</sup>, G. P. Williams<sup>1</sup>

<sup>1</sup>Thomas Jefferson National Accelerator Facility (JLab), 12000 Jefferson Ave., Newport News, VA 23606, USA

<sup>2</sup>Istituto Nazionale di Fisica Nucleare, Via E. Fermi 40, 00044 Frascati, Italy

<sup>3</sup>Brookhaven National Laboratory, Upton, NY 11973, USA

<sup>4</sup>Deutsches Elektronen-Synchrotron, Notkestrasse 85, 22603 Hamburg, Germany

<sup>5</sup>Los Alamos National Laboratory, Los Alamos, NM 87545, USA

<sup>6</sup>University of California Los Angeles, 405 Hilgard Ave., Los Angeles, CA 90095, USA

## Abstract

Commissioning of two large coherent light facilities at SLAC and DESY should begin in 2008 and in 2011 respectively. In this paper we look further into the future, hoping to answer, in a very preliminary way, two questions. First: ‘What will the next generation of the XFEL facilities look like?’ Believing that superconducting technology offers several advantages over room-temperature technology, such as high quality beams with highly populated bunches and the possibility of energy recovery or higher overall efficiency, we focus this preliminary study on the superconducting option. From this belief the second question arises: ‘What modifications in superconducting technology and in machine design are needed, as compared to the present DESY XFEL, and what kind of R&D program is required over the next few years to arrive at a technically feasible solution with even higher brilliance and increased overall conversion of AC power to photon beam power’. In this paper we will very often refer to and profit from the DESY XFEL design, acknowledging its many technically innovative solutions.

## INTRODUCTION

Two high brilliance pulsed XFEL facilities have been proposed: one at SLAC (LCLS) [1] and another at DESY [2] (by a European collaboration). The maximum expected peak brilliance\* of these facilities, at the shortest wavelength of about 1 Å are:  $8.5 \cdot 10^{32}$  and  $5.4 \cdot 10^{33}$  for the SLAC and DESY facilities respectively. The DESY XFEL will provide average brilliance of  $1.6 \cdot 10^{25}$ , (roughly 380 times higher than the facility at SLAC), as a result of different driving linac technologies. However, the single bunch parameters of both designs are quite similar. The maximum final beam energy is 15 GeV in the case of the LCLS and 20 GeV in the case of the DESY XFEL. The charge per bunch is

1 nC and the transverse normalized emittance is  $\sim 1.4 \mu\text{m}\cdot\text{rad}$ . The rms bunch length is 80 fs (DESY) and 97 fs (SLAC). The difference in average brilliance mostly results from the number of bunches per second, which is 120 for the LCLS and 40000 for the DESY XFEL. The superconducting linac of the DESY XFEL allows one to accommodate longer trains of bunches (up to 4000 bunches with a repetition frequency of 10 Hz), even when operated at the maximum energy of 20 GeV.

Recent experimental results of GeV scale energy recovery at JLAB [3] are quite encouraging. This, combined with continuing progress in the performance of superconducting cavities, demonstrated at many laboratories e.g. DESY [4] and JLab [5], initiated our discussions.

Here we explore the feasibility of continuous wave (CW), or semi-CW operational mode for a future XFEL facility. One recognizes that this mode will significantly increase the average brilliance of the XFEL. Pulsed RF systems usually do not allow one to increase the beam on-time, so one has to look for an alternative solution. The only remedy we see in this situation is to operate in the Energy Recovery (ER) mode.

## Energy Recovery at JLab

Last year Jefferson Lab proposed and carried out an energy recovery experiment [3] utilizing CEBAF – the recirculating superconducting accelerator. A schematic representation of the experiment is shown in Fig. 1. Beam is injected into the North Linac (NL) at 20 MeV where it is accelerated to 520 MeV. The beam traverses

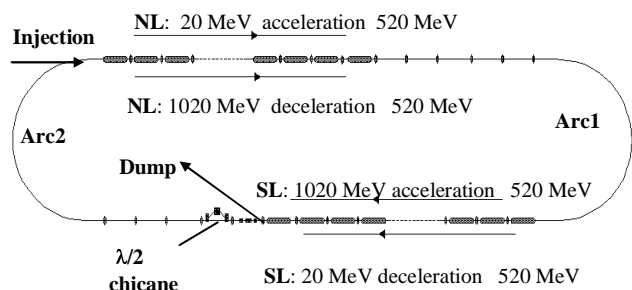


Figure 1: CEBAF Energy Recovery Experiment at JLab.

\* Work supported in part by the U.S. DOE under contract Nr. DE-AC05-84ER40150. This contribution contains studies presented in more detail in publication submitted to PR-ST AB in Fall 2003.

\*Units: photons/s/mm<sup>2</sup>/mrad<sup>2</sup>/0.1% bandwidth.

Arc1 and then is accelerated through the South Linac (SL) where it reaches a maximum energy of 1020 MeV. Following the SL, the beam passes through a newly installed phase delay chicane. The chicane creates a path length differential of exactly  $\frac{1}{2}$ -RF wavelength so that upon re-entry into the NL, the beam is  $180^\circ$  out of phase with the cavities and will be decelerated to 520 MeV. After traversing Arc1 a second time, the beam enters the SL - still out of phase with the cavities - and is decelerated to 20 MeV, at which point the spent electron beam is sent to a dump. The conclusion drawn from this experiment is that there is no limitation preventing energy recovery at higher beam energies, even though the large difference in energy between the two beams at most points in the linacs necessitated the development of compromised lattice settings. Furthermore, measured beam quality characteristics show no degradation of the initial phase space during the energy recovery process. The beam profile is consistent with a Gaussian distribution down to five orders of magnitude in intensity. Later, we will propose an energy recovery option based on the injection of the decelerated beam backwards from the high-energy side to avoid potential problems with optics matching.

### Cryoplant Capacity vs. Pulse Length

Due to cavity dynamic wall losses and long integrated RF on-time, the CW and semi-CW operational modes will require a bigger cryogenic plant than the pulsed option. To keep a reasonable size of the cryoplant for the CW XFEL the following solutions are proposed:

- increase linac length by  $\sim 16\%$  (compared to the present DESY XFEL design)
- operate cavities at  $E_{\text{acc}}$  up to 15 MV/m (nominal operation) and up to  $\sim 22$  MV/m (extended operation)
- operate linac in CW or semi-CW mode (long RF pulse) with adjustable duty cycle vs.  $E_{\text{acc}}$  to stay within available cryogenic budget.

The chosen nominal gradient should ensure high intrinsic quality factor,  $Q_0$ , of the superconducting (sc) cavities. Recent experience with 1.3 GHz TTF<sup>\*</sup> cavities at DESY shows that at 2 K these bulk Nb cavities can be operated at  $E_{\text{acc}}$  up to 20 MV/m without  $Q_0$  degradation. Fourteen cavities from the third production (fifteen were tested) had high  $Q_0$  ( $>1.3 \cdot 10^{10}$ ) up to 22 MV/m. In this paper we will assume that on average  $Q_0$  is  $1.7 \cdot 10^{10}$  at 15 MV/m dropping to  $1.3 \cdot 10^{10}$  at 22 MV/m. An active linac length of 1132 m is needed to reach an energy of 17 GeV (nominal energy of the DESY design) operating cavities at  $E_{\text{acc}} = 15$  MV/m. Taking all this into account the dynamic loss due to the fundamental mode for the whole linac at 2 K would be 16 kW. The above cryogenic load can be significantly lowered if the linac is operated in a semi-CW mode, with a single, long pulse each second. The length of the pulse can be scaled with  $\sim (E_{\text{acc}})^{-2}$ , while maintaining a 1 Hz repetition frequency.

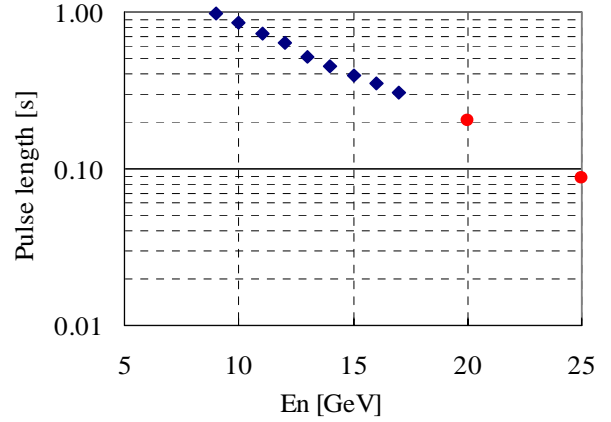


Figure 2: RF pulse length vs. final beam energy  $E_n$ . Nominal range (diamonds), extended range (dots).

If experiments require lower energy photons the linac can be operated at lower gradients and the pulse length can be increased. We propose to use a cryoplant with 8.5 kW capacity at 2 K (including 50 % overhead). This choice is rather arbitrary since the cryoplant capacity can be optimized with respect to variety of parameters, such as: linac length, operation temperature, RF pulse length and capital cost. The chosen cryoplant size is 1/3 of the cryoplant proposed for the TESLA collider [6] and is about the same size as the cryoplant at JLab (5 kW). Fig. 2 shows the maximum beam on-time vs. the final beam energy  $E_n$  when 2/3 of the cryoplant capacity is used. Within the above energy range, the beam on-time varies from 1 s (CW) up to  $E_n = 9$  GeV, 206 ms at  $E_n = 20$  GeV and to 88 ms at  $E_n = 25$  GeV.

## LINAC

A possible layout of the proposed CW facility is quite similar to the present layout of the DESY XFEL. Several components will make the CW facility different from the pulsed version. First of all, the CW facility requires a novel CW RF-gun. Present state-of-the-art RF-guns do not fulfill the performance level needed for a CW XFEL. Vigorous R&D programs, based on a variety of approaches, at BNL, FZ-Rossendorf, Cornell University, Beijing University and at AES, provide optimism that a low emittance ( $1 \mu\text{m-rad}$ ),  $\sim 1$  nC charge/bunch CW RF-gun with a bunch frequency up to a few MHz should be available in the very near future. Another modification is the novel beam transport solution - a 'Teardrop' return arc combined with bypass mini-chicanes to avoid beam-beam interaction.

### RF-Gun and Injector

A very attractive approach has been proposed at BNL [7]. The basic idea is to illuminate the back wall of a superconducting Nb cavity ( $\frac{1}{2}$ -cell) with a UV laser. The niobium performs as the photo-cathode, generating electrons that are accelerated by the RF field of the cavity. The R&D program at BNL is primarily focused on increasing the rather low intrinsic quantum efficiency ( $\eta$ ) of niobium. As was shown experimentally, various

\* TESLA Test Facility

surface treatment, such as: mechanical diamond polishing or/and laser cleaning, can increase  $\eta$  from  $2 \cdot 10^{-7}$  to  $5 \cdot 10^{-5}$ . A further increase of  $\eta$  is possible when the emitting spot is exposed to a high electric field. Any improvement in  $\eta$  is of great importance. Even with  $\eta = 10^{-4}$ , the laser power deposited in the Nb wall while generating a CW beam of several MHz and 1 nC/bunch would probably be too high to keep the illuminated spot superconducting [9]. Fortunately, the emitting spot is exposed to a very low magnetic field which reduces the probability of a quench. In addition, improving  $\eta$  is important because the illuminating laser itself will be technically very challenging. Performance of the proposed injector layout is shown in Fig. 3. In this 15 m long split injector, bunches are accelerated up to 120 MeV. Beam acceleration (gun cavity and eight 9-cell superconducting cavities) and beam focusing (solenoid) take place at different longitudinal positions. The layout opens a new possibility for a high brightness superconducting RF gun [10]. Beam and injector parameters are listed in Table 1.

### General Layout of the ‘Single Arc’ Option

The ‘Single Arc’ scenario is shown in Fig. 4. After bunch shortening in the first bunch compressor, BC I, (from  $\sigma_z = 1.7$  mm to  $\sigma_z = 0.25$  mm, rms) bunches are accelerated to 0.5 GeV and compressed again in BC II to  $\sigma_z = 0.1$  mm. Both compressors are positioned almost as in the original DESY XFEL linac design and thus those designs can be directly adopted. Compression to  $\sigma_z = 0.025$  mm rms in BC III takes place after acceleration to 2 GeV. This compressor needs to be modified, (compared to the original design), to provide separation of accelerated and decelerated beams. This can be accomplished by adding two extra dipole magnets and by proper positioning of the compressor.

The injector and the first part of the accelerator, up to 0.5 GeV, will not be part of the ER ‘loop’. The argument is that the decelerated beam would make an additional contribution to undesired transverse HOMs (already excited by the accelerated beam, which would in turn contribute to emittance degradation of still low energy accelerated beam. This effect will be studied more

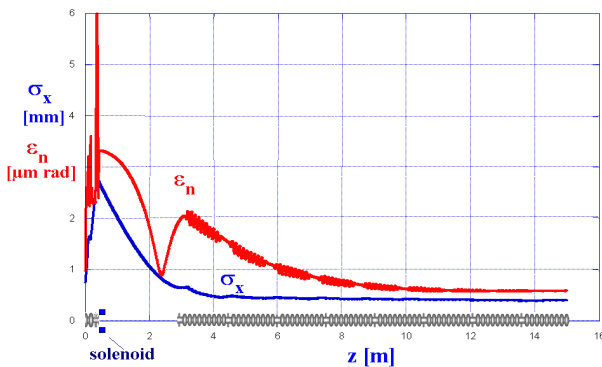


Figure 3: Layout and beam functions of the split injector (acceleration and focusing take place at different longitudinal positions).

Table 1: Parameters of the beam and the injector

Parameter	units	
Cavity operating frequency	MHz	1300
E wall in RF-gun cavity	MV/m	60
Emitting spot radius	mm	1.5
Charge	nC	1
Energy at the end of RF-gun	MeV	6.5
Normalized emittance at the cathode	$\mu\text{m}\cdot\text{rad}$	0.45
B field in the solenoid	T	0.3
Beam energy at the exit	MeV	120
$E_{\text{acc}}$ in eight superconducting cavities	MV/m	13.6
Peak current	A	50
Bunch duration (flat top part)	ps	20
Transversal size, $\sigma_x$ at the exit	mm	0.5
Normalized emittance at the exit	$\mu\text{m}\cdot\text{rad}$	0.6

quantitatively in due course. Assuming an average beam current of 1 mA, 0.5 MW of RF power is needed for the operation of this part of the facility.

The second part of the linac, above 0.5 GeV, has to be operated in the ER mode to lower the RF power needed for operation. All bunches, after passing through optical devices are turned around via a  $180^\circ$  ‘Teardrop’ loop and are injected back into the linac on the high energy side. They are decelerated along the linac until the energy drops to 0.5 GeV. Finally, the returning beam is sent to a dump. Deceleration takes place at the same gradient as acceleration. The main advantage of the injection from the high-energy side is that both accelerated and decelerated beams maintain the same energy profile along the linac, which simplifies the optics design and guarantees uniform periodic focusing for both beams.

### Time Structure of the Beam

Having two beams passing through the second part of the linac in opposite directions one has to avoid beam-beam interaction, which may lead to beam quality degradation for the accelerated beam [11]. With this in mind we propose the following three beam time structures.

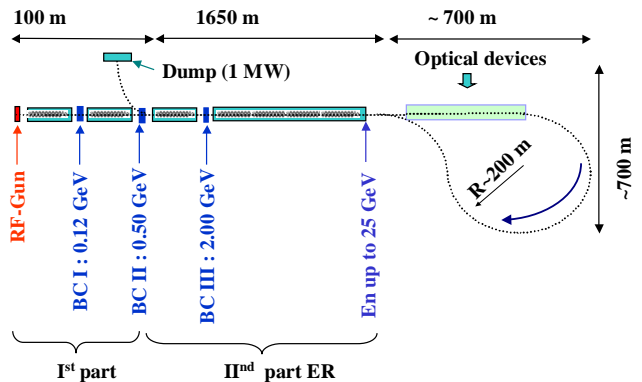


Figure 4: Preliminary layout of the facility based on the single return arc.

### Nominal Beam

The nominal beam will consist of 1 nC bunches with a repetition frequency of 1 MHz (time between two consecutive bunches  $t_b = 1 \mu\text{s}$ ). The ER part of the linac is about 1650 m long, so only six accelerated and six decelerated bunches will be in the ER part at the same time. Bunches of the two beams will meet at twelve locations (see Fig. 5). Lateral separation (of a few millimeters) applied at these locations will be enough to suppress the beam-beam interaction to a negligible level. A single dipole magnet will bend the trajectories of the two counter propagating beams (the accelerated and decelerated beams) in the opposite directions. At the high energy end of the linac the beams will be separated by the last dipole magnet of the return arc. Similarly, at the low energy end the most downstream magnet of the bunch compressor, BC II, will separate both beams appropriately and will also direct the returning beam to the dump. In all other nine locations, beams can be separated via simple bypasses (Fig. 6) based on four dipole magnets. Chicane parameters (for 10 mm horizontal displacement at 15.5 GeV) are listed in Table 2. The magnetic field of the bypass scales linearly with beam momentum. The total length of a bypass chicane with additional space needed for installation between cryostats is about 6 m. All chicanes together extend the linac by 54 m. The linac layout will allow for operation with beams for which  $t_b$  is a multiple of  $1 \mu\text{s}$ . The distance between mid-planes of neighboring bypasses (zone) is 150 m.

### Short Trains of Bunches\*

The proposed bypass chicanes are roughly  $20 \cdot \lambda$  long (distance between the entrance and the exit dipole). They can accommodate trains of up to 20 bunches with the smallest possible spacing of one wavelength ( $\lambda$ ). These short trains of accelerated and decelerated beams will still stay separated in the ER part of the linac. The highest repetition frequency of the short trains is the same as the highest repetition frequency of the nominal beam.

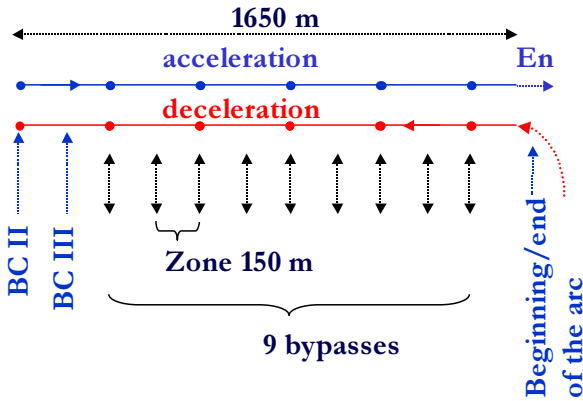


Figure 5: Locations in which the accelerated and the decelerated beams ‘meet’ in the ER part of the linac.

\* a different type of low charge and high frequency RF-gun will be needed to generate above beam structure.

Table 2: Parameters of the bypass chicane for 15.5 GeV

Parameter	Units	
Beam energy	GeV	15.5
Beams separation	mm	20
Chicane length	mm	4630
Dipole magnet length	mm	500
$\theta_{\text{bend}}$	°	0.366
$\rho$	m	78
B	T	0.66
Synchrotron radiation losses:	keV	265
$D_{\text{max}}$	mm	10
$M_{56}$	mm	-0.13

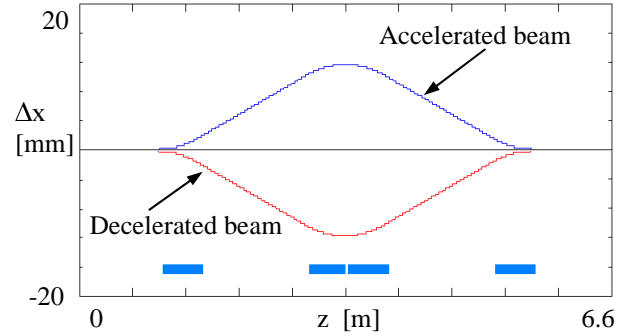


Figure 6: Horizontal displacement of both beams in the bypass chicane (four identical dipole magnets – marked as blue bars).

### Long Train\*

The circumference of the return arc is about 1300 m. It can accommodate (together with the ~700 m long straight beam line needed for collimation system, photon diagnostics and undulators) a  $6.7 \mu\text{s}$  long train of bunches. Such a train, after full acceleration and subsequent passage through all the insertion devices will return back to the linac without encountering any beam-beam interaction. The maximum number of bunches (for bunch spacing of one wave-length) is  $\sim 8700$ . To keep the beam energy constant along the bunch train one has to adjust the phase of consecutive bunches to compensate for the cavity gradient droop (which depends on the total charge of the train). The required phase corrections are small if the total charge (in the train) is of the same order as the charge of the nominal beam passing through the linac within train duration ( $\sim 7 \text{ nC}$ ). In this case, the energy difference between the first and the last bunch in the train will be 31 MeV (for beam energy of 17 GeV). This can be compensated to 8 MeV by a proper phasing of both linac parts (phase correction over the whole train duration is  $3^\circ$ ). Then the next train can be generated and may enter the linac when the last bunch of the previous train reaches the beam dump; the trains can repeat every  $24 \mu\text{s}$ .

### Building blocks

The first part of the linac, up to 0.5 GeV as shown in Fig.5, will operate in a standard accelerating mode (no



ER) and at constant gradient. Thirty-two 9-cell TTF-like cavities operating nominally at 15.2 MV/m are needed to reach that energy. On average, each cavity will transfer 15.6 kW of the RF power to the nominal beam through a fundamental power coupler (FPC). This power level is well below the peak power specified and measured for pulsed operation of the TTF FPCs (240 kW), therefore no multipacting or other voltage induced phenomena in the FPC are expected. The only concern is heating of the FPC due to the larger duty factor. This will require further re-consideration of thermal effects in couplers and it may call for cooling improvements in the present design.

A layout of the ER part of the linac can be configured utilizing the so called superstructures (SST) - “chains” of weakly coupled multi-cell superconducting structures, first proposed in 1999 [12]. In 2002, the first beam test of two cold prototypes was conducted in the TTF linac at DESY, confirming their expected RF properties [13]. This would reduce the number of FPCs in an accelerator (a whole chain is ‘fed’ by only one FPC) and it simultaneously allows for very good damping of HOM’s. RF power transferred to the beam from external sources will be relatively small in the ER part. One can save substantially on the capital cost making the accelerating structures long (with many cells). Here, we propose to use 2x9-cell superstructures (Fig. 7) in the ER part of the

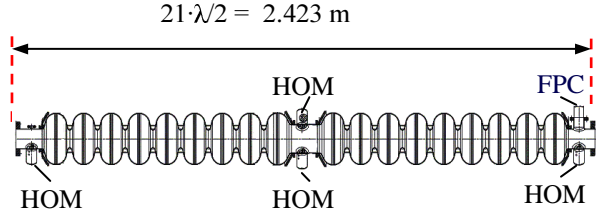


Figure 7: 2x9-cell SST with additional space of  $2 \cdot \lambda/2$  at both sides. Note that these 18 cells are equipped with only one FPC and four HOM couplers.

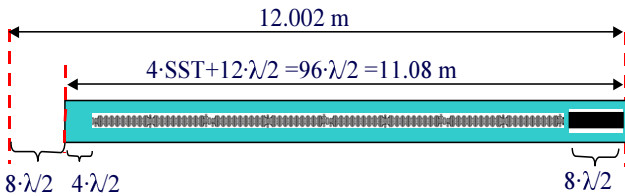


Figure 8: Cryomodule housing 4 SSTs. Space for focusing elements (quads) and BPMs is marked as a ‘black bar’ on the right.

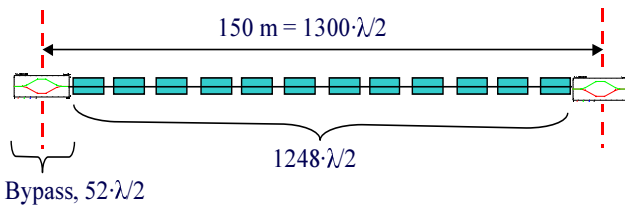


Figure 9: A twelve cryomodule RF zone.

linac. This SST is also proposed as an alternative layout in the TESLA Technical Design Report [14] for the 800 GeV upgrade of the collider. To synchronize both beams with accelerating (decelerating) fields in the linac, the distance between SST’s in the cryomodules is fixed to one  $\lambda$ . Each cryomodule, e.g. based on the DESY design, will house: four SST’s, one quadrupole, a steering coil package and a beam position monitor. The cryomodule is  $48 \lambda$  long and the distance between cryomodules is  $4 \lambda$ . The whole unit is shown in Fig. 8. A 150 m long zone accommodates twelve cryomodules and one bypass chicane as illustrated in Fig.9.

### Energy Recovery

Percentage of energy losses for the entire facility (assuming the nominal beam structure) are collected in Table 3. The net radiation in all photon devices is assumed to be in the range of 2.5 % of the total beam energy. Synchrotron radiation (SR) in the return arc, when arc radius is 200 m, stays below 1.4 %. The synchrotron radiation in the bypass chicanes is negligibly small (even at 25 GeV). The accelerated beam is composed of very short bunches, which increases energy deposition in the parasitic longitudinal modes of cavities. The low frequency part of this power will be transferred to external loads by HOM couplers. Beam line HOM absorbers will absorb the higher frequency part. The longitudinal loss factor  $k_{||}$ , which scales approximately with the bunch length as  $\sim 1/\sqrt{\sigma_z}$ , serves as a measure of energy deposition. For an 18-cell SST, assembled in a multi-structure cryomodule, the average  $k_{||}$  is 40 V/pC (for  $\sigma_z = 0.025$  mm) [15]. The returning beam will also deposit energy into the HOM’s, however its power loss can be significantly reduced by lengthening the bunches. Appropriate optics choices in the return arc architecture (e.g. adjustable momentum compaction by design) will facilitate the above requirements (see section on the arc design). A substantial fraction of the beam energy can be recovered in the second part of the linac (see last row of Table 3). We assume (with a reasonable safety margin) that at least 96 % of the beam energy can still be recovered (in the II-part of the linac), even for 25 GeV operation<sup>\*\*</sup>.

Table 3: Estimated normalized energy loss [in %] for the nominal beam at various energies

Final energy	9 [GeV]	17 [GeV]	25 [GeV]
Total radiation in all ID’s	-2.5	-2.5	-2.5
Return arc SR	-0.06	-0.43	-1.38
All chicanes SR (both beams)	-0.001	-0.008	-0.02
HOMs (both beams)	-0.33	-0.18	-0.12
Energy gain in the I-st part	5.6	2.9	2.0
Max. ER in the II-nd part	<b>100</b>	<b>99.8</b>	<b>98.0</b>

<sup>\*\*</sup> Deceleration off-crest might be needed to compensate for the energy spread.

## Microphonics

Suppression of frequency modulation caused by mechanical cavity vibration (microphonics) is the second crucial technical challenge (following the CW low emittance RF-gun design). According to the estimate presented in [16], 5 kW of RF power will be sufficient to compensate both the “residual” beam loading and microphonics. The facility can operate stably up to 20 GeV, if microphonics do not exceed 16 Hz. Operation at higher energies will require additional RF power, or better suppression of mechanical vibration. Measurements at FZ Rossendorf on TTF cavities [17] showed that proper cryostat construction may lead to an effective reduction of the frequency modulation to 10 Hz (2 Hz rms), as compared to 24 Hz with the original TTF cryostat design [18]. In addition, one can apply an active vibration compensation by means of piezoelectric actuators similarly to the Lorentz force detuning compensation in superconducting cavities [19].

## Linac Parameters

Table 4 summarizes parameters of the first part of the linac (including the injector cryomodule) operating for the nominal beam structure at constant gradient. As was mentioned before this part should operate in the normal accelerating mode (without ER). Parameters of the ER linac are summarized in Table 5. The maximum tolerable peak-to-peak microphonics have been computed assuming a maximum of 5 kW/SST of available generator power. Maximum beam on-time was computed assuming 5.6 kW of 2 K total cryogenic loss in the ER linac. The total loss includes static and dynamic loss coming from the fundamental mode as well as from HOMs excited by the nominal accelerated and decelerated beams. The estimate is based on the cryogenic budget breakdown given in TESLA TDR. The average beam power at the dump is quite moderate. There is no necessity for a dump bigger than 1 MW as long as the total stored charge in the facility does not exceed the one for the nominal beam and the response time of the interlock system is shorter than 100 ms.

Table 4: Parameters of the first part of the linac

Parameter	Units	
Energy at the exit	MeV	500
Input energy	MeV	6.5
Eacc	MV/m	15.2 (13.6)*
Number of 9-cell structures	-	32
f of accelerating mode	MHz	1300
(R/Q)	$\Omega$	1038
Qo	$10^{10}$	1.7
Qext	$10^7$	1.6 (1.5)*
Total cryogenic load at 2 K	kW	0.5
RF power	MW	0.5

\* Gradient and Qext for the injector cryomodule.

Table 5: Parameters of the ER part of the linac

Parameter	Units				
Input beam energy	GeV	0.5			
Type of SST	-	2x9-cell			
f of $\pi$ -0 mode	MHz	1300			
(R/Q)	$\Omega$	1970			
Number of SSTs	-	528			
Number of CMs*	-	132			
Number of zones	-	11			
Number of FPCs	-	528			
Cryo. budget at 2 K	kW	8			
RF budget	kW	2640			
ER ratio	-	0.96			
Energy gain	GeV	8.5	16.5	19.5	24.5
Eacc	MV/m	7.7	15.0	17.8	22.3
Qo	$10^{10}$	1.8	1.7	1.6	1.3
Qext	$10^7$	7.5	7.9	8.0	14.0
Max. p-p $\delta f$	Hz	> 16	> 16	15	9
Beam on-time /s	ms	1000	308	206	88
Number of bunches/s	$10^6$	1	0.308	0.206	0.088
Peak beam power	MW	9	17	20	25
<Power at dump>	MW	0.84	0.36	0.27	0.13

## RF System for the ER Part of the Linac\*

Without ER, 9 to 20 MW of RF power would be needed to operate this part of the linac with nominal beam in the final energy range from 9 to 20 GeV. ER operation significantly reduces this power (to less than 3 MW). Although this level of RF power can easily be supplied by three 1.2 MW klystrons, we do not see this as a practical solution, mainly because of the complicated and expensive distribution system (176 SSTs/klystron) and technical difficulties in controlling amplitudes and phases in all the cavities. One can think of a much more attractive RF system based on 20-25 kW Inductive Output Tubes (IOT). One IOT can be directly attached to one CM housing four SSTs. The gain of these devices is 20-23 dB, so that a 130-200 W amplifier will be needed to drive one IOT. The other, probably more expensive option, is to use 20 kW klystrons. The choice of the RF-system is still an open question, but one may expect substantial capital cost saving, compared to the RF-system of pulsed XFEL.

## RETURN “TEARDROP” RING

The return “Teardrop” ring is based on a periodic triplet focusing structure, which is a smooth continuation of linac FODO focusing. The ring is composed of 120 identical “inward bending” periodic cells and 40 “outward bending” cells closing a 180° ring. The basic

\*Cryomodules.

\* This section is based on study at BNL.

cell architecture (two dipoles and a focusing triplet) is shown in Figure 10 (beta-functions and dispersion). The two kinds of cells differ only in the sign of the horizontal dispersion (mirror reflection). To make the ring achromatic the first/last two cells are different – they have one dipole (right/left) removed in order to zero the horizontal dispersion and its derivative outside the ring. Similarly a three-cell-transition insert is placed at the junction point between the ‘inward-outward’ parts of the ring. The first cell has the ‘right’ dipole removed, in the second one both dipoles are missing and the third cell has the ‘left’ dipole removed in order to ‘flip’ the sign of the horizontal dispersion, while maintaining the periodicity of the Twiss functions. The ring optics has a betatron phase advance per cell of 90 deg. That is preferable from the point of view of chromatic effects compensation. The period length is slightly shorter (about 8 m) than for the linacs to achieve a small value of  $M_{56}$  (of about 64 cm). The crucial beam transport issue is to maintain manageable beam sizes. This calls for short cells and for putting stringent limits on dispersion and beta functions (beam envelope).

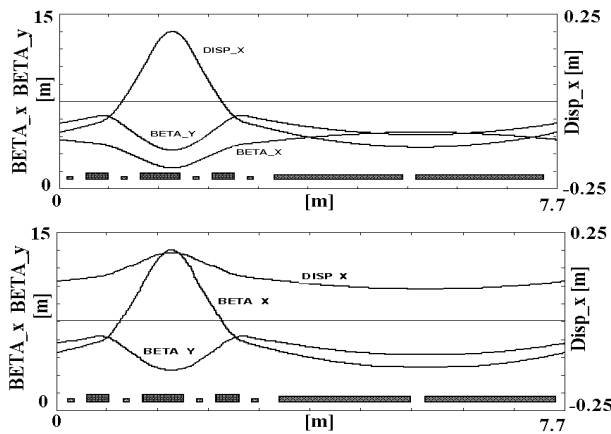


Figure 10: Twiss functions and dispersion of the periodic cells in the return ring. Inward cells (upper diagram), outward cell (lower diagram). Bars illustrate magnets.

## MOTIVATION

### XFEL Operation

One of the attractive aspects of CW operation is the possibility of providing large spacing between FEL pulses, while keeping the total repetition rate high. There seems to be unanimous agreement, that for a pump-probe experiment, synchronization of the FEL facility with a conventional laser is of paramount importance. This means that a 200 ns spacing would be too close, while a 1  $\mu$ s spacing is sufficient for most pump-probe experiments. Furthermore, it is the spacing that allows multiplexing bunches into multiple beam lines, resulting in a larger spacing in the individual beam lines. If we assume 10 beam lines; each beam line may then have a laser synchronized to the beam, running at 100 kHz. For some experiments 10 kHz may be even better.

### Nuclear Physics Operation

Another versatile feature of the proposed XFEL complex is that the driving linac itself, operating in the normal accelerating mode (CW without ER) is capable of delivering electron beams with energies as high as 20 GeV and currents up to 50  $\mu$ A – a very attractive facility for Nuclear Physics studies. The above scenario assumes 5 kW budget of RF power per SST; compensating both the beam loading and microphonics ( $< 14$  Hz). The resulting time structure of the beam would resemble the present beams of the CEBAF accelerator. Such a facility could carry out elements of the nuclear physics program proposed for the 12 GeV CEBAF upgrade. Furthermore, future progress in mechanical vibration suppression will open the additional possibility of an energy upgrade beyond 20 GeV at modest cost.

## R&D PROGRAMS

The scheme presented for a future energy recovery, CW XFEL gives a preliminary answer to our first question. It is a good ‘starting point’ – no ‘show stoppers’ have been found so far. A thorough assessment of collective effects will follow. However, it should undergo further optimization driven by experimental needs as determined by the user community. Obviously a different layout, based on injection of the decelerating beam from the low energy side is also an option. This system will be less demanding on a cavities spacing tolerance. It will require an additional transfer line and two return Teardrop rings at each end of the ER part, if the returning beam line is installed in the same tunnel as the accelerator. This seems to make the ‘Two Arcs’ option more expensive than the one presented. Additionally, the optics and focusing scheme are more challenging but not impossible, as it was recently demonstrated by the CEBAF Energy Recovery Experiment.

### R&D: RF-Gun

The answer to the second question is more complex. This discussion confirms that present R&D programs leading to CW low emittance RF-guns should be continued to take full advantage of the CW operated facility. Increasing Quantum Efficiency of Nb (the BNL approach) and/or testing photo emission from other superconductors (Pb) should be pursued. Furthermore, the use of shorter wave length lasers ( $\lambda < 248$  nm) to illuminate the photo-emitting area should be tested with other superconducting materials.

### R&D: Microphonics

The second R&D topic – microphonics – is directly related to capital and operating costs. Better suppression of microphonics lowers RF system cost, since the required RF budget scales almost linearly with the microphonics amplitude. There has not been much experience with operating multi-cell superconducting cavities when assembled in a multi-structure cryomodule with  $Q_{\text{load}}$  as high as  $7 \cdot 10^7$ – $1.4 \cdot 10^8$ . However, a simple

estimate shows that 5 kW/SST of RF power would be sufficient to operate the ER part of the linac up to 20 GeV. Therefore, there is a significant need for an experimental demonstration of the phase and the amplitude stability control for such high  $Q_{load}$ .

### *R&D: Cavities*

Routinely achievable accelerating gradients in superconducting cavities already exceed gradients needed to operate the CW XFEL facility presented here at beam energies beyond those of both large facilities at DESY and at SLAC. An important improvement in cavity performance is enhancement of intrinsic  $Q$  at the operating gradient. In addition, novel production and preparation methods should ensure its reproducibility and repeatability. Similar to the suppression of microphonics, higher  $Q$  will lower the total cost of the facility (cryoplant costs) and/or will allow for longer beam on-time in the semi-CW operation.

### *R&D: Energy Recovery*

Future ER experiments at CEBAF above 1 GeV energy will be required to confirm that decelerated beam quality can be preserved for higher (than 50) full to injection energy ratio. This is of more importance for the "Two Arcs" option since the "Single Arc" option does not 'suffer' from compromised focusing for very different energy beams.

We notice in passing that all the R&D programs, which are essential to demonstrating feasibility of the CW operated "Single Arc" XFEL facility, are already in progress in many leading Laboratories e.g.: BNL, JLab or DESY.

## SUMMARY AND FINAL REMARKS

Neither capital nor operation costs are expected to be lower than those of the DESY XFEL presented in [2]. Significant savings in the capital cost of the RF system (sources, power supplies and distribution) and cost savings resulting from the SST layout may cover part of the additional costs due to: 16 % more cavities, larger cryoplant and the return "Teardrop" arc. All additional costs are difficult to estimate, at the moment, since they depend strongly on progress in the R&D programs over the next few years. Operation of a future CW facility will require about 9 MW power and the operation costs will be higher than for the pulsed DESY XFEL facility (3.5 MW).

These additional expenses may be justified given the increased performance and flexibility of the proposed facility. The CW XFEL will boost the average brilliance, by a factor of 25 at 9 GeV, or a factor of 5 at 20 GeV (compared to the average brilliance of the pulsed version). Furthermore, it will extend the energy range beyond 20 GeV without additional cost.

## ACKNOWLEDGEMENTS

The authors would like to thank G. Kraft, G. Niel, C. Rode, M. Tiefenbach and G. Wu for providing useful

information included in this paper and for helpful discussions.

## REFERENCES

- [1] Linac Coherent Light Source – CDR, SLAC-R-593, April 2002, Stanford, CA, USA.
- [2] Editors: R. Brinkmann et al., "TESLA XFEL" Technical Design Report- Supplement, DESY 2002-167, TESLA- FEL 2002-09, Hamburg, 2002.
- [3] S. A. Bogacz et al., "CEBAF Energy Recovery Experiment", PAC03, Portland 2003, USA.
- [4] H. Weise, "Superconducting RF Structures- Test Facilities and Results", PAC03, Portland 2003, USA
- [5] P. Kneisel et al., "First Cryogenic Tests with Jlab's New Upgrade Cavities", SRF2003, Lübeck 2003, FRG.
- [6] Editors: R. Brinkmann et al., "TESLA-TDR", DESY, Hamburg, 2001.
- [7] T. Srinivasan-Rao et al., "Design, Construction and Status of All Niobium Superconducting Photo-injector at BNL", PAC03, Portland 2003, USA.
- [8] P. Kneisel, JLAB-TN, to be published.
- [9] T. Schultheiss et al., "Thermal/Structural analysis of a SCRF Photocathode Electron Gun Cavity", PAC03, Chicago 2001, USA.
- [10] M. Ferrario et al., "An Ultra-high Brightness, High Duty Factor, Superconducting RF Photoinjector", to be published.
- [11] D. Douglas, "Incoherent Thoughts about Coherent Light Source", JLAB-TN-98-040, 1998.
- [12] J. Sekutowicz et al., "Superconducting Superstructure for the TESLA Collider; A Concept", PR-ST AB, 1999.
- [13] J. Sekutowicz et al., "Cold- and beam test of the first prototypes of the superstructure for the TESLA collider" PAC03, Portland 2003, USA.
- [14] R. Brinkmann et al., "TESLA Technical Design Report, Part II: The Accelerator", DESY 2001-01, Hamburg, March 2001.
- [15] R. Brinkmann et al. , "Terahertz Wakefields in Superconducting Cavities of the TESLA-FEL Linac", TESLA Report 2000-07, DESY, 2000.
- [16] L. Merminga, J. Delayen, "On the Optimization of Qext under Heavy Beam Loading and in the Presence of Microphonics", JLAB TN-96-022.
- [17] A. Büchner et al. "Noise Measurements at the RF System of the ELBE Superconducting Accelerator", PAC03, Portland 2003, USA.
- [18] M. Liepe, "Superconducting Multicell Cavities for Linear Collider", DESY-Thesis-2001-045, October 2001, Hamburg, FRG.
- [19] M. Liepe et al., "Dynamic Lorentz Force Compensation with Fast Piezoelectric Tuner", PAC01, Chicago 2001, USA.